Injection and transport of electric charge in a metal/copolymer structure*

Li Dong-Mei(李冬梅)[a)†], Yuan Xiao-Juan(袁晓娟)[a)], Ma Jia-Sai(马嘉赛)[a)], and Liu De-Sheng(刘德胜)[a)b)]

[a)] *School of Physics, State Key Laboratory of Crystal Materials, Shandong University, Jinan* 250100, *China*

[b)] *Department of Physics, Jining University, Qufu* 273155, *China*

(Received 28 January 2011; revised manuscript received 24 June 2011)

The dynamical processes of the electric charge injection and transport from a metal electrode to the copolymer are investigated by using a nonadiabatic dynamic approach. The simulations are performed within the framework of an extended version of the one-dimensional Su–Schrieffer–Heeger (SSH) tight-binding model. It is found that the electric charge can be injected into the copolymer by increasing the applied voltage. For different structures of the copolymer, the critical voltage biases are different and the motion of the injected electric charge in the copolymer varies obviously. For the copolymer with a barrier-well-barrier configuration, the injected electric charge forms a wave packet due to the strong electron–lattice interaction in the barrier, then comes into the well and will be confined in it under a weak electric field. Under a medium electric field, the electric charge can go across the interface of two homopolymers and enter into the other potential barrier. For the copolymer with a well-barrier-well configuration, only under strong enough electric field can the electric charge transfer from the potential well into the barrier and ultimately reach a dynamic balance.

Keywords: injection and transport, electron–lattice interactions, potential barrier, potential well

PACS: 72.80.Le, 73.40.Gk, 71.35.Ee **DOI:** 10.1088/1674-1056/20/11/117203

1. Introduction

Since the discovery of the first thin-film organic light-emitting devices (OLEDs),[1] there has been much interest in improving their performance due to their enormous potential for making highly visible flat large area colour displays.[2,3] In those electronic devices, conjugated polymers are used as the light-emitting and the electric charge-transporting layers, in which electrons and/or holes are injected from the metal electrode and driven by the external field. The injection and the transport of the charge carriers are essential factors for determining the properties of the OLEDs and have been central points of studying the mechanisms of those devices.[4−8] Due to the strong electron–lattice interactions, it is well known that the injected electrons or holes are in self-trapping states called polarons or bipolarons as the transport carriers in the conjugated polymers.

Compared with the organic conjugate polymer, the copolymer can enhance the photo- and the electroluminescent efficiencies of the LEDs by increasing conductivities of both electrons and holes and by the interfacial confinement of the excitons.[9,10] On the other hand, the functionality of the copolymer can be easily tailored by using chemical synthesis, molecular design and self-assembly to be suitable for a particular application.[11−13] So an effective strategy for enhancing the device efficiency is to employ the copolymer instead of the homopolymer as the active component.[14,15] Poly (*p*-phenylene) (PPP), which has higher conductibility, heat resistance, well air stability and doping property, is difficult to liquate and manufacture. However, for poly-thiophene (PT), which has higher conductibility, stability and dissolvability, the effect of the heteroatom sulfur on the π–conjugated electron makes the thiophene an important material in the application of technology. Therefore it has guiding significance for the organic material, especially for the light-emitting material, to study the electronic property of the copolymer that is composed

*Project supported by the National Basic Research Program of China (Grant No. 2009CB929204), the National Natural Science Foundation of China (Grant No. 11074146), the Natural Science Foundation of Shandong Province, China (Grant Nos. ZR2010AM037 and ZR2010AM026), and the Independent Innovation Foundation of Shandong University, China (Grant No. 2009TS097).

†Corresponding author. E-mail: li_dm@sdu.edu.cn

© 2011 Chinese Physical Society and IOP Publishing Ltd

of PPP and PT. By studying the electronic and the light absorption properties of the copolymer, Kanemistu *et al.*[16] have shown that –(PT)$_n$–PPP–(PT)$_n$– has a typical trap-barrier-trap structure, the light-emitting property of the copolymer can be controlled by changing the conjugated length of the trap and the configuration of the barrier. The electronic structure of diblock copolymers is studied in the framework of an inter-component coupling model. It is found that the band gap can be tuned by changing the proportion of the homopolymers. The interfacial coupling between the components can also affect the band gap obviously.[17] The quantum well and the superlattice characteristics of the quasi-one-dimensional multiblock copolymers are described within the framework of the tight-binding model. The quantum tunneling, the Franz–Keldysh effect and the quantum confinement can be generated under an applied electric field.[18] Because of the abundant characteristics and the more extensive applications of the copolymer, in this paper, we present our results from a nonadiabatic dynamical study on the evolution of the electronic states in a metal/copolymer system. We discuss the transport of the injected electric charge in a metal/copolymer structure under an external field.

2. Model and method

Consider a one-dimensional metal/copolymer structure, the configuration of the copolymer is $-$(PPP)$_m$–(PT)$_n$–(PPP)$_m$–, which is attached to the end of a metal electrode. The model is shown in Fig. 1. Due to the characteristics of PPP and PT, the CH group is regarded as coupling coordinate u_n, which moves along the chain; the π electron of sp^2 is described by the tight-binding model; the electron–lattice coupling is described based on the non-adiabatic approximation; the electron–electron interaction is neglected. It has been shown that the electron–lattice interaction predominates in the properties of the polymers, if the electron–electron interaction is not too strong. Under the fixed bound condition, we deduce the extended Su–Schrieffer–Heeger (SSH) model to describe the injection and the transport of the electric charge in the system.

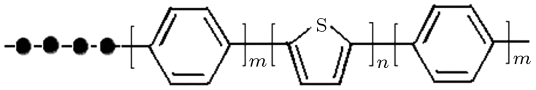


Fig. 1. Model of metal/copolymer.

The Hamiltonian is composed of three parts

$$H = H_{\rm e} + H_{\rm latt} + H_{\rm ext}. \tag{1}$$

The Hamiltonian of the electronic part is

$$H_{\rm e} = -\sum_n \varepsilon_n C^+_{n,\sigma} C_{n,\sigma} + H_{\rm M} + H_{\rm C}, \tag{2}$$

where ε_n denotes the on-site electronic energy on a lattice site (CH group) and $C^+_{n,\sigma}$ ($C_{n,\sigma}$) denotes the electron creation (annihilation) operator at site n with spin σ ($\sigma =\uparrow, \downarrow$); The $H_{\rm M}$ and $H_{\rm C}$ are the electronic part Hamiltonians of the metal electrode and the copolymerand, respectively, and can be written as

$$H_{\rm M} = -\sum_n t_0 (C^+_n C_{n+1} + C^+_{n+1} C_n), \tag{3}$$

$$\begin{aligned} H_{\rm C} = & -\sum_n^N \left[t_0(n) - \alpha(n)(u_{n+1} - u_n) - t_1 \cos\frac{n\pi}{2} \right] \\ & \times \left(C^+_{n+1} C_n + C^+_n C_{n+1} \right) \\ & - \sum_n^N t_2 \left(C^+_{4n-3} C_{4n} + C^+_{4n} C_{4n-3} \right) \\ & + \sum_n^N t_3 (C^+_{4n} C_{4n} + C^+_{4n-3} C_{4n-3}), \end{aligned} \tag{4}$$

where t_0 denotes the hopping integral between the nearest neighbouring carbon atoms of the unpolymerized chain, α is the electron–lattice coupling constant between the neighbouring sites, u_n is the coordinate displacement of the n-th site from its equidistant position, t_1 is introduced to lift the ground-state degeneracy of the nondegenerate polymer and t_2 and t_3 are the contributions of the sulphur atom. In PPP, $t_2 = t_3 = 0$; in PT, $t_2 \neq 0$, $t_3 \neq 0$.

The Hamiltonian due to the lattice distortion in the copolymer is

$$H_{\rm latt} = \frac{K}{2} \sum_n (u_{n+1} - u_n)^2 + \frac{M}{2} \sum_n \dot{u}_n^2, \tag{5}$$

where K denotes the elastic constant and M is the mass of a CH group.

The contribution from the external electric field is

$$H_{\rm ext} = \sum_{n,\sigma} V_n(\tau) \left(C^+_{n,\sigma} C_{n,\sigma} - 1 \right), \tag{6}$$

where τ denotes time, $V_n(\tau)$ is the lift potential energy of the metal electrode for the electric charge injection, $V_n(\tau) = V(\tau)$, or the driving field for the moving of the injected electric charges in the copolymer, $V_n(\tau) = -|e| E(\tau) [(n - n_0) a + u_n]$, with $E(\tau)$ being

the applied electric field, e the electric charge, n_0 the first site of the copolymer and a the lattice constant.

The interfacial coupling between the copolymer and the metal electrode is described by the hopping integral $t_{\mathrm{M-P}} = \beta_1 t_0$, where β_1 is the coupling parameter. It has been indicated that the interface with coupling strength $\beta_1 < 1$ acts as a potential barrier and the injected electric charge tends to depart from the interface, while the interface with $\beta_1 > 1$ acts as a potential well and the injected electric charge tends to be confined at the interface.[19] Due to the softness of the organic polymers, it is easy to form a self-adjusting interface between the polymer and the contact electrode. Therefore, the interface can be optimized to realize an effective electric charge injection in organic devices. In this paper, we choose $\beta_1 = 0.4$.

The interfacial coupling parameters between the polymers in the copolymer are

$$\begin{aligned} t_0^{\mathrm{PPP/PT}} &= \frac{\beta_2}{2}\left(t_0^{\mathrm{PPP}} + t_0^{\mathrm{PT}} - t_1^{\mathrm{PPP}} \cos\frac{n_{\mathrm{PPP}}\pi}{2} \right. \\ &\quad \left. - t_1^{\mathrm{PT}} \cos\frac{n_{\mathrm{PT}}\pi}{2}\right), \\ \alpha^{\mathrm{PPP/PT}} &= \frac{\beta_2}{2}\left(\alpha^{\mathrm{PPP}} + \alpha^{\mathrm{PT}}\right), \\ K^{\mathrm{PPP/PT}} &= \frac{\beta_2}{2}\left(K^{\mathrm{PPP}} + K^{\mathrm{PT}}\right), \end{aligned} \tag{7}$$

where superscript PPP/PT denotes the interface between the PPP and the PT, PPP and PT denote the PPP and the PT parts, respectively, and β_2 is the coupling constant between two polymers. It is found that an interface with a weak coupling serves as an energy barrier and that with a strong coupling as a well, both of which can significantly affect the intrachain process in the copolymers.[20] The interfacial coupling parameter is chosen to be $\beta_2 = 1.0$ as an average coupling in this paper.

The wave function of an electron is $|\Phi_{\mu,\sigma}(\tau)\rangle = \sum_{n,\sigma} \Psi_{\mu,\sigma}(n,\tau)\,|n\rangle$. The evolution of the electronic state is obtained by solving the time-dependent Schrödinger equation

$$\begin{aligned} &\mathrm{i}\,\hbar\dot{\Psi}_{\mu,\sigma}(n,\tau) \\ &= -t_n \Psi_{\mu,\sigma}(n+1,\tau) - t_{n-1}\Psi_{\mu,\sigma}(n-1,\tau) \\ &\quad - t_2 \Psi_{\mu,\sigma}(n+3,\tau)\,\Delta\left(\frac{n+3}{4},\mathrm{int}\right) \\ &\quad - t_2 \Psi_{\mu,\sigma}(n-3,\tau)\,\Delta\left(\frac{n}{4},\mathrm{int}\right) \\ &\quad - t_3 \Psi_{\mu,\sigma}(n,\tau)\left(\Delta\left(\frac{n}{4},\mathrm{int}\right) + \Delta\left(\frac{n+3}{4},\mathrm{int}\right)\right) \\ &\quad + V_n(\tau)\,\Psi_{\mu,\sigma}(n,\tau), \end{aligned} \tag{8}$$

where

$$\Delta(i,\mathrm{int}) = \begin{cases} 1, & i = \text{integer}, \\ 0, & \text{otherwise}, \end{cases}$$

site index n runs over the whole chain.

Classically, lattice displacement $\{u_n\}$ of the system is determined by the Newtonian equations of motion

$$\begin{aligned} M\ddot{u}_n(\tau) &= -K\left(2u_n(\tau) - u_{n+1}(\tau) - u_{n-1}(\tau)\right) \\ &\quad + 2\alpha\left(\rho^{\sigma}_{n,n+1}(\tau) - \rho^{\sigma}_{n-1,n}(\tau)\right) \\ &\quad + |e|\,E(\tau)\left[\rho^{\sigma}_{n,n}(\tau) - 1\right], \end{aligned} \tag{9}$$

where site index n runs only in the copolymer chain, $\rho^{\sigma}_{n,n'}$ is the element of the density matrix and is defined as

$$\rho^{\sigma}_{n.n'}(\tau) = \sum_{\mu,\sigma} \Psi^{*}_{\mu,\sigma}(n,\tau)\, f_{\mu,\sigma} \Psi_{\mu,\sigma}(n',\tau), \tag{10}$$

with $f_{\mu,\sigma}$ being the time-independent distribution function determined by the initial occupation (0, 1, or 2). The coupled differential equations (9) and (10) can be solved numerically with the Runge–Kutta method of order 8 with the step control.[21] It has been widely used and proven to be an effective approach in the study of the dynamics in the conjugated polymers.

The dynamical evolution starts from the system with a static structure, which is given by the static lattice configuration obtained through minimizing the total energy of the system

$$\begin{aligned} &u_{n+1} - u_n \\ &= \frac{1}{2}\left\{u_{n+1} + u_{n-1}\right. \\ &\quad + \frac{2\alpha}{K}\sum_{\mu}{}'[\Psi_{\mu,\sigma}(n+1,t=0)\,\Psi_{\mu,\sigma}(n,t=0) \\ &\quad \left. - \Psi_{\mu,\sigma}(n,t=0)\,\Psi_{\mu,\sigma}(n-1,t=0)]\right\}. \end{aligned} \tag{11}$$

We consider a finite one-dimensional metal/copolymer system with a 70-site metal electrode and a 200-monomer copolymer chain ($m = 72$, $n = 56$), which is long enough for the present investigation. The parameters of the models for PT and PPP are chosen from the experiments and the numerical work in the static state to be[22,23] $t_0 = t_0^{\mathrm{PPP}} = t_0^{\mathrm{PT}} = 2.5$ eV, $t_1^{\mathrm{PPP}} = 1.0$ eV, $t_1^{\mathrm{PT}} = 0.675$ eV, $t_2 = t_3 = 0.125$ eV, $\alpha^{\mathrm{PPP}} = \alpha^{\mathrm{PT}} = 4.5$ eV/Å, $K^{\mathrm{PPP}} = K^{\mathrm{PT}} = 21.0$ eV/Å^2, $a = 1.22$ Åand $M = 1349.14$ eV $\cdot$ fs^2/Å^2. The on-site energy of the metal layer is assumed to be zero, which means that the Fermi level of the metal is almost in the middle of the band gap of the copolymer. Therefore, the highest occupied electronic state

is confined in the metal electrode before an external field is applied.

In the calculation, we assume that the external bias is turned on smoothly, that is, $V(\tau) = V_0 \exp\left[-(\tau-\tau_c)^2/\tau_w^2\right]$ for $0 < \tau < \tau_c$ and $V(\tau) = V_0$ for $\tau \geq \tau_c$, with τ_c being a smooth turn-on period and τ_w the width. The applied electric field $E(\tau)$ is also turned on smoothly in the same mode, i.e., $E(\tau) = E_0 \exp\left[-(\tau-\tau_c)^2/\tau_w^2\right]$. In the calculations, we take $\tau_c = 30$ fs and $\tau_w = 25$ fs, and various values of voltage bias V_0 and E_0.

3. Result and discussion

3.1. Copolymer with barrier-well-barrier configuration

In this section, we consider the composition of the copolymer with the –$(PPP)_m$–$(PT)_n$–$(PPP)_m$- structure in the metal/copolymer system. The PPP has a wide band gap of about 2.73 eV between the highest occupied molecular orbital (HOMO) and the lowest unoccupied molecular orbital (LUMO), while the PT has a narrow band gap of about 2.26 eV. When the PPP and the PT are combined to form the copolymer, the gap of the PT will fall into that of the PPP. This kind of copolymer [–$(PPP)_m$–$(PT)_n$–$(PPP)_m$–] will have a typical alternate barrier-well-barrier structure. At $t = t_0$, the structure of the metal/copolymer system is obtained by solving the static Schrödinger equation with the equilibrium condition by iteration. The Fermi level of the metal is assumed to be in the middle of the gap of the PPP by setting $\varepsilon_n = 0$ as stated above.

In this paper, the staggered lattice configuration is described by $y_n = (-1)^{n+1}(2u_n - u_{n+1} - u_{n-1})/4$, which expresses the lattice structure of the copolymer. When $\tau = 0$ fs, $y_n \approx 0.04$ Å. The injected electric charge distribution is shown by $\rho_n = \rho_{n,n} - 1$. When $\tau = 0$ fs, $\rho_n = 0$. For convenience, we smoothly treat y_n and ρ_n as $y'_n = (y_{n-1} + y_n + y_{n+1} + y_{n+2})/4$ and $\rho'_n = (\rho_{n-1} + \rho_n + \rho_{n+1} + \rho_{n+2})/4$, respectively.

Firstly, we present our results of the electric charge injection under a weak applied electric field of $E_0 = 5.0 \times 10^3$ V/cm. In this case, it is found that the electric charge is apparently injected into the PPP chain through the metal/copolymer interface when the critical voltage bias about 1.29 eV is applied. Although the bias is lower than the LUMO of the PPP, due to the existence of the virtual polaron level in the metal/copolymer system,[24] the electric charge can be injected into the PPP layer when the Fermi level of the metal is just above the virtual polaron level. However, in the real system, this virtual polaron level does not exist before the electron injection. The values of m and n can also influence the injection of the electric charge. It is found that when the length of the copolymer is a constant, the band gap of the copolymer can be broadened as the PPP proportion increases; and the gap of the copolymer can be narrowed if the PT proportion increases.[25] So the critical voltage bias for injecting the electric charge can rise (decline) as the value of m (n) increases.

The evolution of the total injected electric charge distribution is shown in Fig. 2. It is easily found that the whole injection process lasts about 1000 fs and the quantity of the electric charge injected into the copolymer chain is about $1.0e$, while only $0.7e$ stays in the PPP chain. Because the gap of the PPP is greater than that of the PT, part of the injected electric charge can go across the interface of PPP/PT and come into the PT chain under the effect of the electric field. However, the applied electric field is too weak, the injected electric charge cannot entirely enter into the PT chain.

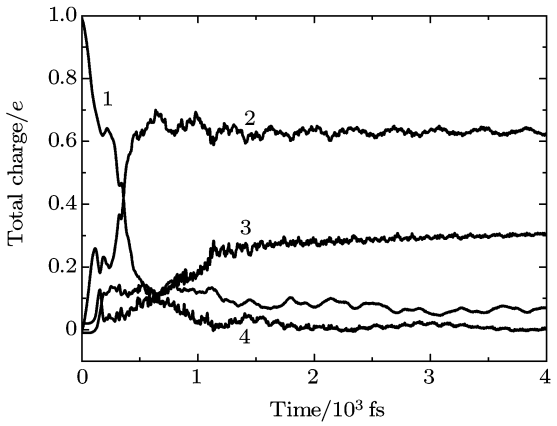


Fig. 2. Variations of total electric charge with time under $E_0 = 5.0 \times 10^3$ V/cm and $V_0 = 1.29$ eV, with 1, 2, 3 and 4 denoting the metal electrode, the left PPP chain, the PT chain and the right PPP chain, respectively.

Figure 3 shows electric charge distribution ρ'_n and lattice configuration y'_n at a few typical time for the weak field case. It is found that about $0.5e$ is injected into the PPP layer after 305 fs, forming a small wave packet because of the electron–lattice interaction. In addition, a small quantity of electric charge comes into the PT chain and induces the tiny lattice vibration (see Fig. 3(a)). Then after about 650 fs, about $0.9e$ is injected into the PPP chain, forming a

big wave packet; about $0.1e$ is injected into the PT chain, forming a small wave packet (see Fig. 3(b)). Afterwards, the transport of the electric charge comes to stabilization, the injected electric charge forms a very stable but small wave packet in each of the PPP and the PT chains (see Figs. 3(c) and 3(d)).

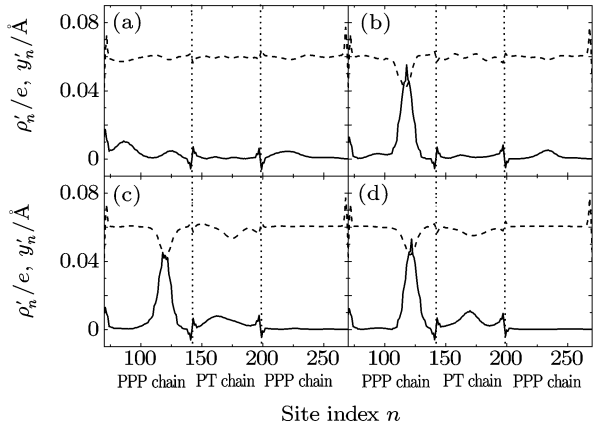


Fig. 3. Variations of electric charge distribution ρ'_n and staggered lattice configuration y'_n of the $-(\mathrm{PPP})_m-(\mathrm{PT})_n-(\mathrm{PPP})_m-$ chain with site index under $E_0 = 5.0 \times 10^3$ V/cm and $V_0 = 1.29$ eV at (a) $\tau = 305$ fs, (b) $\tau = 650$ fs, (c) $\tau = 1200$ fs and (d) $\tau = 2000$ fs. The region in between the two dot lines denotes the PT chain and the two side regions of the dot lines denote the PPP chains.

Then we increase the electric field at the same voltage bias. It is found that when the electric field goes up to $E_0 = 4.0 \times 10^4$ V/cm, the injected electric charge comes into the PT chain. Figure 4 shows the evolution of the total injected electric charge distribution under the critical electric field. With the evolution of time, the quantity of the electric charge in the left PPP chain gradually increases to about $0.7e$, then slowly reduces to zero; the quantity of the electric charge in the PT and the right PPP chains gradually increases. This phenomenon illuminates that part of the electric charge injected into the PT chain can overcome the interface barrier of PT/PPP under the effect of the electric field, transfer into the PPP chain and induce a lattice distortion.

Figure 5 shows electric charge distribution ρ'_n and lattice configuration y'_n at a few typical time in the copolymer chain under $E_0 = 4.0 \times 10^4$ V/cm and $V_0 = 1.29$ eV. By comparison with Fig. 4, it is found that the quantity of the electric charge in the left PPP chain reaches a maximum ($0.6e$) after 355 fs and forms a bigger wave packet. At the same time, only a small quantity of the electric charge is injected into the PT chain and induces a tiny lattice vibration. However, there is a lack of the electric charge that is injected into the right PPP chain (see Fig. 5(a)). After 650 fs, the quantity of the electric charge in the left PPP chain gradually decreases, the quantity of the electric charge increases to $0.5e$ in the PT chain and forms a bigger wave packet. At the same time, $0.3e$ goes across the PT/PPP interface, forming a small wave packet in the right PPP chain (see Fig. 5(b)). With the time elapsing, the electric charge in the left PPP chain is entirely injected into the PT chain, the quantity of the electric charge in the PT chain reaches a maximum ($0.6e$) and that in the right PPP chain retains the stabilization (see Figs. 5(c) and 5(d)).

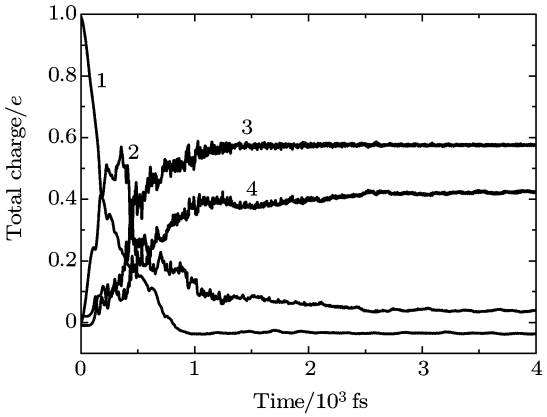


Fig. 4. Variations of total electric charge with time under $E_0 = 4.0 \times 10^4$ V/cm and $V_0 = 1.29$ eV, with 1, 2, 3 and 4 denoting the metal electrode, the left PPP chain, the PT chain and the right PPP chain, respectively.

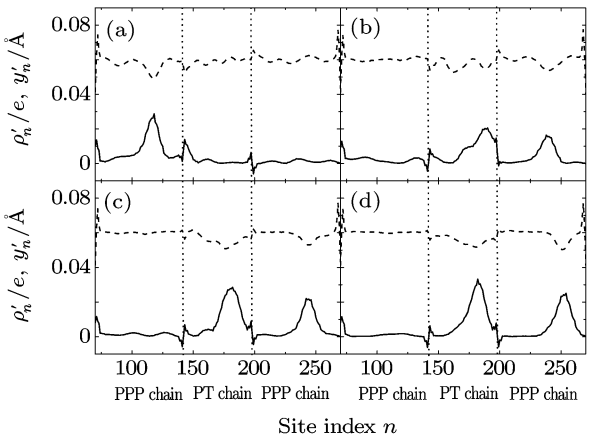


Fig. 5. Variations of electric charge distribution ρ'_n and staggered lattice configuration y'_n of the $-(\mathrm{PPP})_m-(\mathrm{PT})_n-(\mathrm{PPP})_m-$ chain with site index under $E_0 = 4.0 \times 10^4$ V/cm and $V_0 = 1.29$ eV at (a) $\tau = 355$ fs, (b) $\tau = 650$ fs, (c) $\tau = 945$ fs, and (d) $\tau = 1200$ fs. The region in between the two dot lines denotes the PT chain, and the two side regions of the dot lines represent the PPP chains.

Figure 6 shows the time-dependent distribution of the injected electric charge in the copolymer chain. The figure intuitively shows the transport of the electric charge.

When the electric field is increased to an even stronger intensity, e.g., $E_0 = 2.0 \times 10^5$ V/cm, the evolution of the total injected electric charge distribution

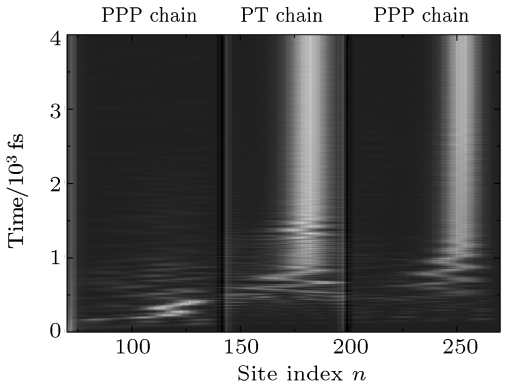


Fig. 6. Variation of electric charge distribution with time in the $-(\mathrm{PPP})_m-(\mathrm{PT})_n-(\mathrm{PPP})_m-$ chain under $E_0 = 4.0 \times 10^4$ V/cm and $V_0 = 1.29$ eV.

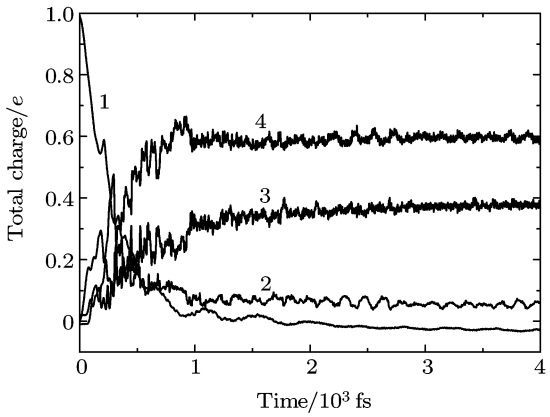


Fig. 7. Variations of total electric charge with time under $E_0 = 2.0 \times 10^5$ V/cm and $V_0 = 1.29$ eV, with 1, 2, 3 and 4 denoting the metal electrode, the left PPP chain, the PT chain and the right PPP chain, respectively.

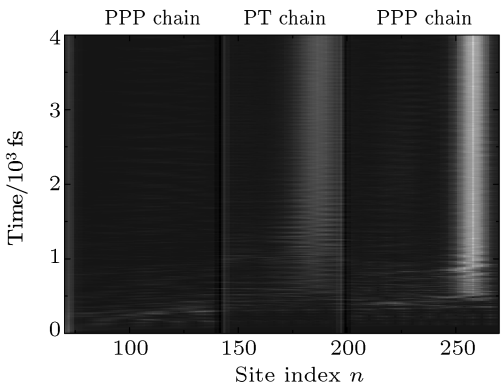


Fig. 8. Variations of charge distribution with time in the $-(\mathrm{PPP})_m-(\mathrm{PT})_n-(\mathrm{PPP})_m-$ chain under $E_0 = 2.0 \times 10^5$ V/cm and $V_0 = 1.29$ eV.

is shown in Fig. 7. With the time elapsing, the injected electric charge first transports from the left PPP chain to the PT chain, then the great mass of the electric charge goes across the PT/PPP interface and comes into the right PPP chain, finally attains the stability. Figure 8 shows the distribution of the injected electric charge varying with time. Under the stronger electric field, the injected electric charge rapidly moves into the copolymer chain and cannot form a stable wave packet in each of the left PPP chain and the PT chain. Finally, the injected charge is restricted to the end of the right PPP chain, inducing an obvious lattice distortion.

3.2. Copolymer with well-barrier-well configuration

In this section, we consider the configuration of the copolymer with the $-(\mathrm{PT})_m-(\mathrm{PPP})_n-(\mathrm{PT})_m-$ structure in the metal/copolymer system. Because of the difference of the band gaps of the homopolymers, this kind of copolymer chain will have a typical alternate well-barrier-well structure.

Firstly, we present our results of the electric charge injection under a weak applied electric field of $E_0 = 5.0 \times 10^3$ V/cm, the critical voltage bias applied to the metal electrode is 0.97 eV. Figure 9 shows the evolution of the total net electric charge of the system. At about 139 fs, the reduced quantity of the electric charge of the metal electrode is about $0.5e$ (curve 1 of Fig. 9). At 700 fs, the quantity of the electric charge hold in the copolymer chain is $1e$. Then after 1100 fs, the electric charge reaches the left of the PT chain. However, the injected electric charge will localized in the left PT chain and cannot enter into

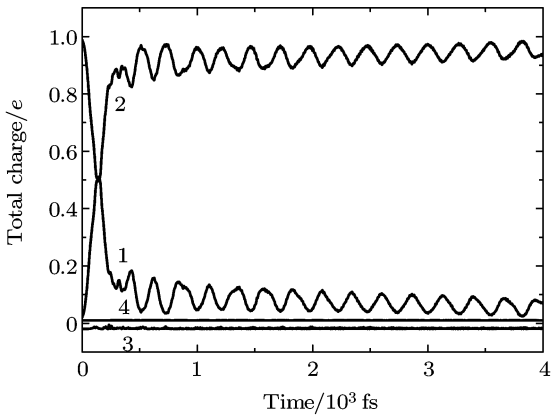


Fig. 9. Variations of total electric charge with time under $E_0 = 5.0 \times 10^3$ V/cm and $V_0 = 0.97$ eV, with 1, 2, 3 and 4 denoting the metal electrode, the left PT chain, the PPP chain and the right PT chain, respectively.

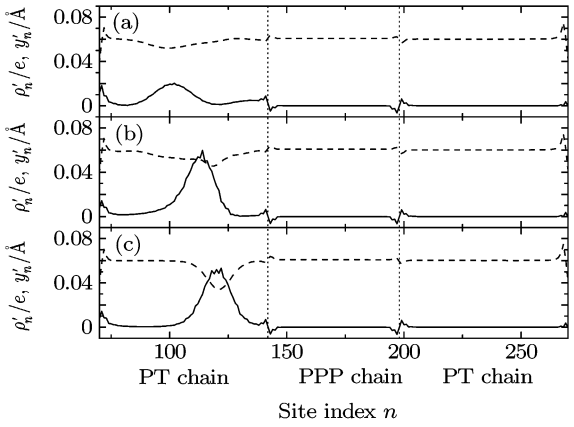


Fig. 10. Variations of electric charge distribution ρ'_n and staggered lattice configuration y'_n of the –(PT)$_m$–(PPP)$_n$–(PT)$_m$– chain with site index under $E_0 = 5.0 \times 10^3$ V/cm and $V_0 = 0.97$ eV at (a) $\tau = 130$ fs, (b) $\tau = 700$ fs and (c) $\tau = 1100$ fs. The region in between the two dot lines denotes the PPP chain, the two side regions of the dot lines represent the PT chains.

the PPP chain. The reason is that the energy of the injected electric charge is too small to overcome the potential barrier of the PT/PPP interface. Electric charge distribution ρ'_n and lattice configuration y'_n of the copolymer chains at a few typical time under this electric field are shown in Fig. 10. The injected electric charge forms a stable wave packet in the left PT chain, which should be a polaron.

When the electric field is increased to a medium intensity, e.g., $E_0 = 4.0 \times 10^4$ V/cm, the evolution of the total net electric charge of the system with time is shown in Fig. 11 and the electric charge distribution varying with time is shown in Fig. 12. In this case, the time when $1e$ is injected into the copolymer is about 350 fs. However, the injected electric charge is still restricted to the left PT chain as in the case of $E_0 = 5.0 \times 10^3$ V/cm.

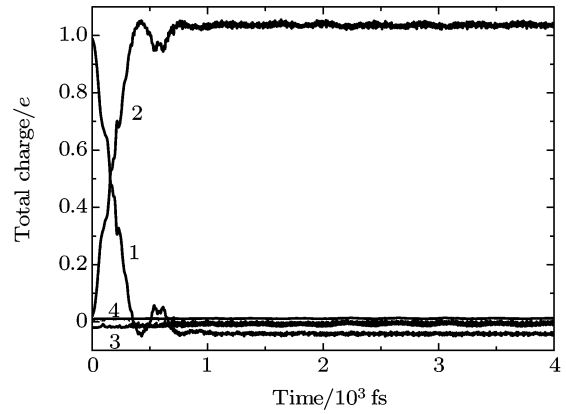


Fig. 11. Variations of total electric charge with time under $E_0 = 4.0 \times 10^4$ V/cm and $V_0 = 0.97$ eV, with 1, 2, 3 and 4 denoting the metal electrode, the left PT chain, the PPP chain and the right PT chain, respectively.

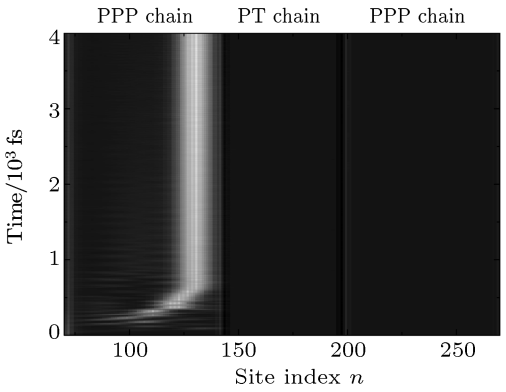


Fig. 12. Variations of electric charge distribution with time in the –(PT)$_m$–(PPP)$_n$–(PT)$_m$– chain under $E_0 = 4.0 \times 10^4$ V/cm and $V_0 = 0.97$ eV.

When the electric field is increased to 4.0×10^5 V/cm, the injected electric charge can cross over the PT/PPP interface and enter into the PPP chain. The evolution of the total net electric charge of the system is shown in Fig. 13. Electric charge distribution ρ'_n and lattice configuration y'_n of the copolymer chain at a few typical time under this electric field are shown in Fig. 14. A comparison between the two figures shows that the injected electric charge forms a wave packet, rapidly moves in the left PT chain and reaches the PT/PPP interface after about 260 fs. However, only a small quantity of electric charge is transported into the PT chain and induces a tiny lattice vibration (see Figs. 13 and 14(a)). At 450 fs, $0.4e$ is localized in the PT chain, $0.2e$ is transfered into the PPP chain (see Figs. 13 and 14(b)). The reason is that the PPP chain is a potential barrier, the PT chain is a well, so the electric charge in the PPP chain can easily enter into the right PT chain, forming a small wave packet (see Figs. 13, 14(c) and 14(d)).

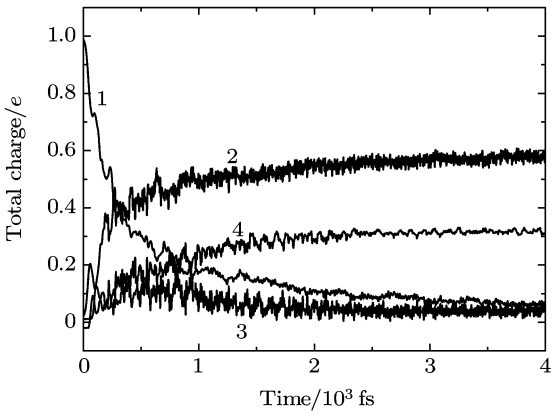


Fig. 13. Variations of total electric charge with time under $E_0 = 4.0 \times 10^5$ V/cm and $V_0 = 0.97$ eV, with 1, 2, 3 and 4 denoting the metal electrode, the left PT chain, the PPP chain and the right PT chain, respectively.

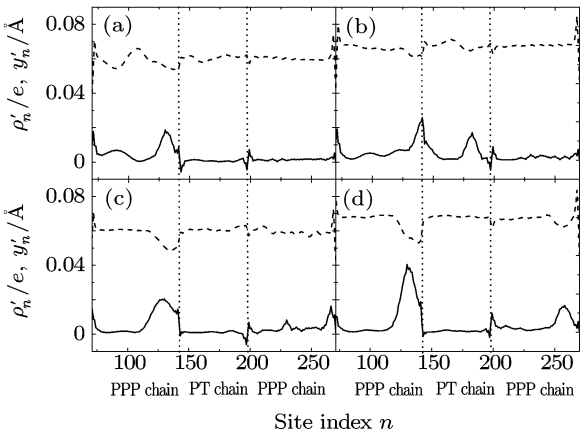


Fig. 14. Variations of electric charge distribution ρ_n' and staggered lattice configuration y_n' of the $-(\mathrm{PT})_m-(\mathrm{PPP})_n-(\mathrm{PT})_m-$ chain with site index under $E_0 = 4.0 \times 10^5$ V/cm and $V_0 = 0.97$ eV at (a) $\tau = 260$ fs, (b) $\tau = 450$ fs, (c) $\tau = 996$ fs and (d) $\tau = 1945$ fs. The region in between the two dot lines denotes the PPP chain and the two side regions of the dot lines represent the PT chains.

4. Conclusion

We analyse the dynamic processes of the electric charge injection and transport in an open metal/copolymer structure using a nonadiabatic method. It is shown that the electric charge can be injected from the electrode into the copolymer layer by adjusting the voltage bias of the electrode. The critical potential voltage and the behaviour of the injected electric charge carrier are related to the configuration of the copolymer. For the copolymer with the barrier-well-barrier configuration, the injected electric charge first forms a wave packet, then transports from barrier to well under the weak electric field, but will be localized in the well. For a moderate electric field, the injected electric charge goes across the interface between two homopolymers into the other barrier. For the copolymer with the well-barrier-well configuration, only when the electric field is strong enough can the injected electric charge transfer from well into barrier and reach the dynamic balance. These conclusions indicate that the copolymer has a quantum confinement effect and, moreover, offers a theoretic reference for the fabrication of the OLEDs based on the copolymer materials.

References

[1] Tang C W and VanSlyke S A 1987 *Appl. Phys. Lett.* **51** 913

[2] Burrows P E, Shen Z, Bulovic V, Mccarty D M, Forrest S R, Cronin J A and Thompson M E 1996 *J. Appl. Phys.* **79** 7991

[3] Shen Z, Burrows P E, Bulovic V , Forrest S R and Thompson M E 1997 *Science* **276** 2009

[4] Cao G H, Qin D S, Guan M, Zeng Y P and Li J M 2008 *Chin. Phys.* B **17** 1912

[5] Brütting W, Berleb S and Mückl A G 2001 *Org. Electron.* **2** 1

[6] Li D M, Li H H, Li Y, Liu D S and Xie S J 2008 *Acta Phys. Sin.* **57** (in Chinese)

[7] Sun Q M, Gao C M, Zhao B X and Rao H B 2010 *Chin. Phys.* B **19** 118103

[8] Gao K, Xie S J, Li Y, Yin S, Liu D S and Zhao X 2009 *Chin. Phys.* B **18** 2961

[9] Liu D S, Wang L X, Xie S J, Han S H and Mei L M 2003 *Chin. Phys.* **12** 548

[10] Lee J I, Zyung T, Miller R D, Kim Y H, Jeoung S C and Kim D 2000 *J. Mater. Chem.* **10** 1547

[11] Tian R Y, Yang R Q, Peng J B and Cao Y 2002 *Chin. Phys.* **14** 1032

[12] Bakhshi A K and Bhargava P 2003 *J. Chem. Phys.* **119** 13159

[13] Zhang L Y, Wang P Y and Shi A C 2009 *Sci. China Phys.* **52** 518

[14] Burn P L, Holmes A B, Kraft A, Bradley D D C, Brown A R, Friend R H and Gymer R W 1992 *Nature* **356** 47

[15] Aarnio H, Westerling M, Osterbacka R, Svensson M, Andersson M R and Stubb H 2006 *J. Chem. Phys.* **321** 127

[16] Kanemistu Y, Suzuki K, Masumoto Y, Tomiuchi Y, Shiraishi Y and Kuroda M 1994 *Phys. Rev.* B **50** 2301

[17] Liu D S, Mei L M, Xie S J and Han S H 2000 *J. Phys.: Condens. Matter* **12** 4333

[18] Liu D S, Wan L X, Wei J H, Han S H and Xie S J 2003 *Sci. China. Ser.* G **46** 417

[19] Fu J F, Ren J R, Liu X J, Liu D S and Xie S J 2006 *Phys. Rev.* B **73** 195401

[20] Li Y, Gao K, Sun Z, Yin S, Liu D S and Xie S J 2008 *Phys. Rev.* B **78** 014304

[21] Brankin R W, Gladwell I and Shampine L F, Compure of RKSUITE, Software for ODE IVPS, http://www.netlib.org

[22] Kobayashi M, Colaneri N, Boysel M, Wudl F and Heeger A J 1985 *J. Chem. Phys.* **82** 5717

[23] Xie S J, Han J S, Ma X D, Mei L M and Lin D L 1995 *Phys. Rev.* B **51** 11928

[24] Stoneham A M, Ramos M M D, Almeida A M, Correia H M G, Ribeiro R M, Ness H and Fisher A J 2002 *J. Phys.: Condens. Matter* **14** 9877

[25] Liu D S, Xie S J and Han S H 2000 *Acta Phys. Sin.* **49** 1556 (in Chinese)